Robustness Comparison of Color Image Watermarking Schemes in Uniform and Non-uniform Color Spaces

Kuo-Cheng Liu[†, ††] **and Chun-Hsien Chou**[†]
[†]Department of Electrical Engineering, Tatung University, Taiwan
[†, ††] Foreign Language and Information Educating Center, Taiwan Hospitality & Tourism College

Summary
Watermarking technique is to hide a sequence of random numbers or a recognizable binary pattern, or the so-called digital watermark, into the media for authorized uses. Color image watermarking even plays an important role due to distributed, manipulated and forged behaviors over networks. In this paper, robustness comparison of color image watermarking schemes using different color spaces for embedding is undertaken. The color watermarking scheme implemented in this paper is to select the signal with high perceptual redundancy for transparent watermark embedding in the wavelet domain. Binary watermark signals are repeatedly embedded into the selected wavelet coefficients by the way of quantization index modification. The watermarking scheme utilizing perceptually redundant signal spaces in both uniform and non-uniform color spaces for hiding watermarks are conducted to compare the corresponding robustness of the embedded watermark. Experimental results of the comparison show that the non-uniform color space can provide a certain part of color signals a large amount of perceptual redundancy for hiding high-strength watermark signals. The watermark embedded in the non-uniform space is always robust than that embedded in the uniform space.

Key words:
Color image watermarking, perceptual redundancy, uniform color space, non-uniform color space.

1. Introduction

The watermarking schemes embed specified information into the media to identify the rightful ownership, disseminated path and allowed users of the original content. Many studies investigated watermarking schemes for images because of the rapid development of the network environment. In the image watermarking scheme, effective exploitation of visual characteristics of human perception is helpful to the design of transparent and robust watermarking schemes [1]. In the past few years, many watermarking schemes incorporated with perceptual knowledge were proposed to embed watermark into the host image [2-6]. The design of the watermarking schemes takes either the sensitivity of the human visual system (HVS) or the masking effects into account. However, most researches pay attention to the development of watermarking schemes for grayscale images. Only some researches have considered watermark hiding in color images.

In [7], a wavelet-based perceptual watermarking scheme for grayscale images was extended for color images by embedding the watermark signal into the brightness component. In [8], authors embedded the watermark by modifying a selected set of pixels in the blue channel, since the human eye is less sensitive to changes in this color channel. In [9], a model of human color vision was used to embed the watermark in the yellow-blue channel of the opponent-color representation of color images and to ensure the embedded watermark is invisible. Caramma *et al*. [10] used different sensitivities of the HVS to the red, green, and blue channels to tune the watermark strength in the proposed color image watermarking scheme. In [11], an image complexity and perceptibility model was proposed to search the interesting regions for casting the watermark in the YUV channels. Barni *et al*. [12] exploited the characteristics of the HVS and the correlation between RGB color channels to hide the watermark into frequency domain of color images and reliable retrieve it. In [13], the insertion and the detection were applied on each color component of the RGB color space. The insertion consists in modifying one vector for each location, with regards to the bit value and the vectors triplet. In [14], a watermarking approach was presented for hiding the watermark into DC components of the color image directly in the spatial domain, followed by a saturation adjustment technique performed in RGB space. Lin *et al*. [15] proposed a novel approach, based on the properties of histograms, to measure the numerous global features of all pixels in a cover image and to construct the three-dimensional feature space. The feature space is dynamically partitioned to identify several blocks used to embed the watermark. In [16], color watermarks are carried by the quantization indices of the host image in the CIELAB color space. It can be found that the knowledge of human visual perception to the difference between colors in different color spaces is not considered for color image watermarking scheme.

Since the HVS has a limited sensitivity in perceiving visual information, it is well believed that there exists quite an amount of perceptual redundancy in color images. The perceptual redundancy of a particular color is represented by the perceptually indistinguishable color

Manuscript received July 5, 2007
Manuscript revised July 25, 2007

region in which each color cannot be distinguishable with the color. That is, the perceptual color difference in the perceptually indistinguishable color region is close to zero. Through making the embedded watermarks be part of the perceptual redundancy in color images, watermark insertion can be achieved with transparency. In this paper, the characteristics of human visual perception to the difference between colors in different color spaces are discussed. The perceptual redundancy inherent in color images of different color spaces is estimated based on the estimation of numerical color difference in the uniform color space. The extent of the perceptual redundancy of a color varies with the color space where it is represented. With the varying volume of perceptually indistinguishable color region in different color spaces, a watermarking scheme based on the perceptual redundancy is implemented and the corresponding results of robustness of the watermarking scheme are compared. The rest of the paper is organized as follows. In Section 2, the relationship of perceptual redundancy inherent in color images among different color spaces is introduced. The watermarking scheme based on the perceptual redundancy is presented in Section 3. The simulation results and the conclusions are described in Section 4 and 5, respectively.

2. Perceptual Redundancy in Color Images among Different Color Spaces

Any color in a color space can be represented by colorimetry as a triplet of numbers called tristimulus values. Colors with different tristimulus values within a color space are perceptually indistinguishable, indicating that perceptual redundancy is inherent in color images. The perceptual redundancy of a color can be quantitatively measured by calculating the distance between that color and each of all possible colors that can be barely differentiated from it by visual perception. However, colors in many color spaces, such as RGB, XYZ, YUV, and YC_bC_r, are not uniformly distributed in the sense that equal perceptual differences between colors correspond to equal distances in the tristimulus space [17]. The estimation of perceptual redundancy in terms of perceptually indistinguishable region for each color in these non-uniform color spaces is complicated.

One main issue in estimating the perceptual redundancy of a target color in color images is that a number of representative color samples, which are just discernible from the color, are needed to define the perceptually indistinguishable region of the color. Since the perceptual color difference between colors in the non-uniform color space depends on the contents of the image and is not correlated with the numerical color difference (or Euclidean distance), the non-uniformity makes pixel-wise threshold estimation virtually impossible. By using the method proposed in [24], a number of representative color samples for a target color are found in the uniform color space. The perceptually indistinguishable region can be approximately defined by exploiting the transformed color samples found in the uniform color space without having to directly assess the perceptual color difference in the non-uniform color space.

Suppose a color space is perceptually uniform, the perceptual color difference between any two colors can be ideally represented as the Euclidean distance between their coordinates. This uniformity of a perceptually uniform color space can be used to quantify the perceptual redundancy of each color in the target color space as the threshold for perceptible color difference. The color space CIELAB is a perceptually uniform color space created by nonlinear transformations of tristimulus XYZ values to overcome the non-uniformity of color spaces that had been discussed by MacAdam [18], [19]. A useful rule of thumb in this color space is that any two colors can be distinguished if their color distance is greater than 3.0 [18].

$$\Delta E_{Lab} = \left(\Delta L^2 + \Delta a^2 + \Delta b^2\right)^{1/2} \geq 3.0 \qquad (1)$$

This distortion threshold is called the just noticeable color difference (JNCD) threshold. The locus of colors that are perceptually indistinguishable from a given color (the locus of discrimination) forms a sphere around that color's coordinates in the space, and such perceptually indistinguishable spheres would have the same radius of JNCD in all regions of the color space.

It is noted that the JNCD threshold was originally obtained by matching homogeneous color samples without following any apparent pattern. Meanwhile, it is found that the perceptibility of color difference depends on the contents of the image [20], [11]. For a color signal in a complex image, the associated threshold of JNCD can be increased by considering its local properties. The JNCD threshold is changed by the human visual system's inconsistent sensitivity to varying stimuli from neighboring pixels in color images. Since the luminance contrast sensitivity function (CSF) is significantly higher than the chromatic CSF [22], only luminance-dominated properties of the HVS, from data in the spatial domain, are employed to adjust the JNCD value of each color signal in this paper. By considering the masking effect mainly due to local variations in luminance magnitude, the threshold of just-noticeable color difference can be set to be larger than JNCD. In this paper, the adaptive JNCD (AJNCD) for each color pixel of color images is measured according to its local image properties in luminance. Using uniformity in the CIELAB color space, the relationship between JNCD and AJNCD of a color pixel in the color image is expressed as

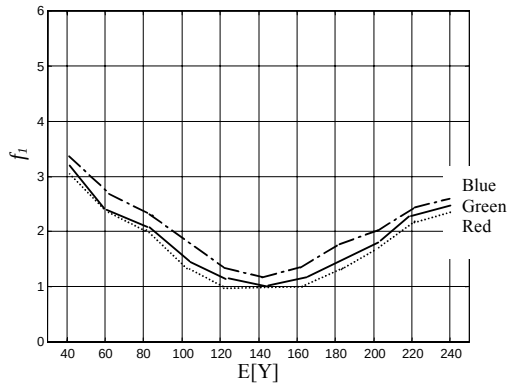

Fig. 1 The relationship between the weighting f_1 and the average background luminance, $E(Y)$.

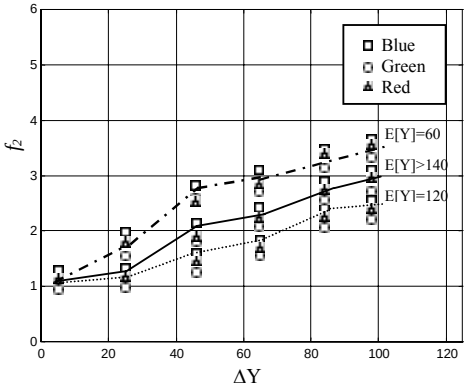

Fig. 2 The relationship between the weighting f_2 and the luminance gradient, ΔY, under different average background luminance, $E(Y)$.

$$AJNCD(\Delta Y, \mathrm{E}[Y]) = w(\Delta Y, \mathrm{E}[Y]) \cdot JNCD \quad (2)$$

where $w(\Delta Y, \mathrm{E}[Y])$ is a weighting function between JNCD and AJNCD while luminance-dominated masking effects are considered. In this paper, two experiments that are similar to those conducted in [23] are designed to measure the perceptually indistinguishable region of each color due to the masking effect caused by human eyes. One of the experiments to be tested is the one considering the average background luminance behind the pixel. The other is the spatial non-uniformity of the background luminance. The former addresses that effect caused by the inconsistency in sensitivity of the HVS to stimuli of varying levels of contrast. That is, the human visual perception is sensitive to luminance contrast rather than absolute luminance value. The later, which is known as texture masking, focuses on the effect caused by spatial non-uniformity of the background luminance. Therefore, the weighting function is modeled as follows.

$$w(\Delta Y, \mathrm{E}[Y]) = \min\{ f_1(\mathrm{E}[Y], f_2(\Delta Y, \mathrm{E}[Y])) \quad (3)$$

where $\mathrm{E}[Y]$ is the average background luminance and ΔY is the maximum weighted average of luminance difference around each pixel in images. The weighting function due to the contrast masking effect is given by f_1. The numerical results are shown in Fig. 1. In our experiments, background intensity dominated by the luminance component is considered in estimating the AJNCD threshold. Different colors, including red, green, and blue, are chosen for the test. A small squared region, 16×16pixels, is located in the center of a flat field with a constant background color which is changed with 10 increments between 40 and 240 in the corresponding luminance magnitude. For each background color, the color noises are randomly added to or subtracted from the color pixels in squared region. By varying the intensity of the color noises in the small squared region, the error visibility threshold for each background color is determined when the perturbed squared region is just noticeable. f_2 represents the weighting function due to the texture masking effect. The closely linear behavior is shown in Fig. 2. In our experiments investigating the texture masking of color signals, background color and spatial non-uniformity dominated by the luminance component are considered in estimating the AJNCD threshold. The edge of each test color is changed with 20 increments between 0 and 120, and the associated background color is changed with 10 increments between 20 and 240 in the corresponding luminance magnitude. Both a perturbed edge and an unperturbed edge are shown to subjects. In the experiments, noises of adjustable amplitude are randomly added to the two-pixel wide regions next to the boundary between two rectangular color patches having the specified luminance difference and mean value, and arbitrary chrominance. The perturbation in each color component is varied until it becomes perceptible. In the above experiments used to measure luminance-dominated adjustment, two-alternative forced choice (2AFC) procedure is adopted to measure detection thresholds for individual color stimuli. By alternately displaying the color patch and its noise contaminated color patch in a rate of 2~8 frames per second, the AJNCD threshold for individual color stimuli can be estimated while the viewers can only see one patch without noticing any change occurred within the alternate patches shown on display monitor at a viewing distance of 6 times the height of the image patch. The type of the monitor is a 21″ SUN CRT monitor of model GDM-5410 with the resolution of 1880×1400.

To estimate the perceptual redundancy of a target color pixel in the target color space, the strategy is to transform this color pixel to the CIELAB color space for measuring the associated AJNCD sphere and then to select color

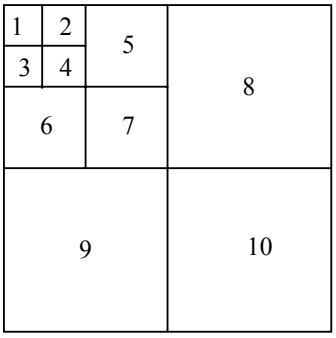

Fig. 3. The numbering of subbands in three-level wavelet decomposition.

samples that are on the surface of the AJNCD sphere [24]. The representative color samples that are just distinguished from the target color pixel are then mapped back to the non-uniform color space to obtain the perceptually indistinguishable region of the target color. Finally, the estimated just noticeable distortion (JND) of the target color for three color components in the target color space are conservatively obtained by taking the minimal distance between target color and those mapping color samples along each color axis. The perceptual redundancy of a color image in any target color space can then be estimated.

To evaluate the perceptual redundancy of each coefficient in the wavelet subband, the component JND profile of the subband in each color component must be obtained. In this paper, the component JND profile of each subband in the color image is obtained by allocating full-band distortion energy in accordance with the CSF of the HVS to spatial frequencies involved in each subband [23]. By using the property of sensitivity to spatial frequencies, a weighting function derived from computing the average sensitivity value of each subband can be utilized to dispense the full-band JND energy to each subband. For the subband decomposition with 3-level wavelet transformation, the weighting function for distributing full-band distortion energy to subband b in luminance is defined as

$$\omega_{\mathrm{Y},b} = \frac{S_{\mathrm{Y},b}^{-1}}{\sum_{k=0}^{9} S_{\mathrm{Y},k}^{-1}}, \qquad \text{for } 1 \le b \le 10 \tag{4}$$

where $S_{\mathrm{Y},b}$ represents the average sensitivity of the HVS to spatial frequencies in the b-th subband of luminance component. The numbering of subbands in the wavelet decomposition is shown in Fig. 3. Since the weighting function of each subband is a normalized desensitivity of the corresponding spatial frequencies and the CSF for luminance signals is significantly higher than the CSFs for chromainance signals, the weighting functions for chrominance components can be also evaluated by Eq. (4).

3. Watermark Embedding and Extraction

In the proposed watermarking scheme, the wavelet coefficient with high perceptual redundancy is selected for watermark embedding. The perceptual significant signals have a perceptual capacity that allows the watermark to be inserted without perceptual degradation [2]. The processes of embedding and extracting the watermark are based on quantizing the wavelet coefficients. The image with the watermark embedded is actually the dequantization of a quantized image, whose quantization indices are disturbed by watermark information. The same watermark is separately embedded into each color channel as in [5]. The choice to embed the watermark in three channels can be used not only to extract the watermark by cooperating with a majority-vote decision process, but also to recover the watermark while the watermarked image is changed to grayscale. The proposed technique can also be applied to single channel images.

With component JND profiles, visual significance of each wavelet coefficient in each subband of each color channel can be evaluated, perceptually significant coefficients in both the luminance and chrominance channels are separately located for watermark embedding. Since perceptually significant coefficients are sparsely distributed in each subband of each color component in the image, each wavelet subband is therefore partitioned into non-overlapping blocks to effectively locate the area with high density of perceptually significant coefficients for watermark insertion. The subband image is first partitioned into non-overlapping blocks, with a block size of 8×8 for bands 1 – 4, 16×16 for bands 5 –7, and 32×32 for other subbands. All blocks are then classified as important or unimportant, depending on the number of significant signals in a block. The blocks in each color channel of the host image are scanned row-by-row in order of increasing subband number for importance classification. The scheme classifies a block as important if more than half of its coefficients are significant. A coefficient in a block is regarded as significant if its associated JND value is greater than the mean JND value for all coefficients in the block. That is, a significant wavelet coefficient will provide a larger perceptually indistinguishable region for tuning the watermark strength without resulting in perceptual distortion. Important blocks are those most likely to be located for embedding.

To guarantee the transparency of the embedded watermark, the difference between the wavelet coefficients of an image and its watermarked counterpart must not result in perceptible distortion throughout the whole image

Fig. 4 Original watermark pattern of size 20×40.

in the spatial domain. To attain this goal, quantization of wavelet coefficients must be carried out with the quantizer step size tuned to result in an imperceptible difference between any two adjacent coefficients in the quantized space. In the proposed scheme, uniform quantization is separately designed for each selected block where each coefficient is quantized by a specified quantizer step size. By analyzing the distribution of JNDs in important blocks, the dynamic range of JNDs is evaluated and exploited to select important blocks for watermark insertion. An important block is selected to embed the watermark if the block's range of JND values is narrow and the variance of all its coefficients' JNDs is less than a predefined threshold. The uniform quantizer of the selected block may be designed with a possibly maximum quantizer step size such that the quantization error and distortion caused by modifying the quantization index will not be perceptible. The step size of the selected block is determined by the minimum value of its coefficients' JNDs.

The watermark is embedded by modifying the quantization index of the wavelet coefficient. A coefficient $r_i(x,y)$ in the *i-th* selected block of each color channel is transformed into a quantization index $q_i(x,y)$.

$$q_i(x,y)=\mathbf{Q}_i(r_i(x,y)) \tag{5}$$

where $\mathbf{Q}_i$ represents the uniform quantization for the block with a step size tuned by its coefficients' JNDs. Applying a modulo-2 operation to the quantization index, $q_i(x,y)$, maps it to a binary form.

$$\hat{q}_i(x,y) = q_i(\mathrm{x},\mathrm{y}) \bmod 2 \tag{6}$$

The binary index provides the space for embedding the watermark. The modification of the binary index for inserting a watermark signal w_k into the given coefficient is

$$q_i^*(x,y) = \begin{cases} q_i(x,y) + \hat{q}_i(x,y) \oplus w_k, & \text{if } \hat{q}_i(x,y) \neq w_k \\ q_i, & \text{otherwise} \end{cases} \tag{7}$$

Watermark extraction is achieved in the sense that the quantization index of the wavelet coefficients in watermarked images is mapped to a binary form. In this way, extracting the watermark from each channel of a color image is straightforward. That is

$$w_k = q_i^*(\mathrm{x},\mathrm{y}) \bmod 2 \tag{8}$$

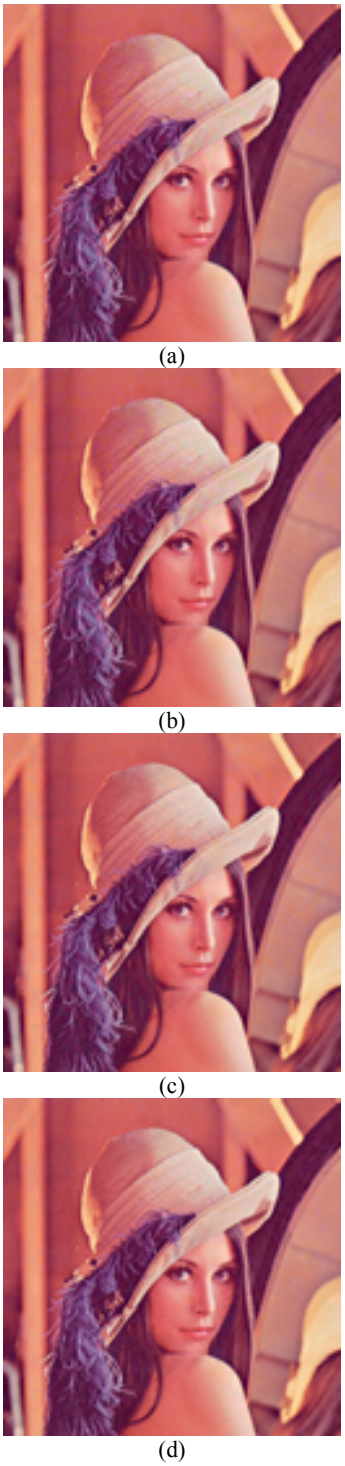

(a) (b) (c) (d)

Fig. 5 (a) Original "Lena" image, (b) the watermarked "Lena" image in the YC_bC_r color space, PSNR=40.38dB, (c) the "Lena" watermarked image in the XYZ color space, PSNR=40.99dB, (d) the watermarked "Lena" image in the CIELAB color space, PSNR=41.44 dB.

(a)

(b)

(c)

(d)

Fig. 6 (a) Original "Goldhill" image, (b) the watermarked "Goldhill" image in the YC_bC_r color space, PSNR=44.37dB, (c) the watermarked "Goldhill" image in the XYZ color space, PSNR= 41.88dB, (d) the watermarked "Goldhill" image in the CIELAB color space, PSNR=42.18 dB.

Since the objective of this paper is to compare the robustness of the watermarking scheme implemented in uniform and non-uniform color spaces, the portability of the key information for watermark extraction, including the location of each selected block and the associated quantization step size, is not discussed in this paper.

Table I The bit error rate of the watermark that is extracted from the attack version of various watermarked images, in each of which watermark is embedded in YC_bC_r, XYZ, and CIELAB color spaces.

Attack	Image	Color space		
		YC_bC_r	XYZ	CIELAB
JPEG compressing	Lena	4.25%	7.88%	16.25%
	Boaats	1.88%	9.65%	13.13%
	Goldhill	5.25%	5.63%	10.25%
	Tulips	6.25%	6.88%	12.38%
Low-pass filtering	Lena	0.00%	0.00%	0.75%
	Boaats	0.00%	0.75%	2.38%
	Goldhill	0.00%	0.00%	0.50%
	Tulips	0.13%	0.38%	1.38%
Noise adding	Lena	1.13%	2.50%	12.88%
	Boaats	2.88%	9.88%	13.38%
	Goldhill	5.88%	6.38%	14.50%
	Tulips	3.50%	5.50%	10.63%
Scaling down	Lena	0.00%	0.00%	0.50%
	Boaats	0.20%	0.25%	1.13%
	Goldhill	0.00%	0.00%	0.00%
	Tulips	0.00%	0.13%	0.50%
Scaling up	Lena	0.38%	0.88%	1.13%
	Boaats	0.38%	1.13%	3.13%
	Goldhill	0.00%	0.00%	0.88%
	Tulips	0.88%	0.75%	6.38%

4. Simulation Results

In the simulation, color images of size 512×512 are used as host images where each pixel was represented by 24 bits in the RGB color space, while the watermark image of size 20×40 contained visually recognizable patterns. The watermark is shown in Fig. 4. To compare the performance of the proposed watermarking scheme in terms of robustness, one uniform color space (CIELAB space) and two non-uniform color spaces (XYZ and YC_bC_r space) are chosen for hiding watermarks to compare the robustness of the embedded watermark. For each color space, the watermark is inserted into luminance channel (Y and L channels) 4 times and other two channels 2 times, respectively. By considering that the watermark is repeatedly inserted into channel Z of a host image n_Z times, a space of n_Z dimension,

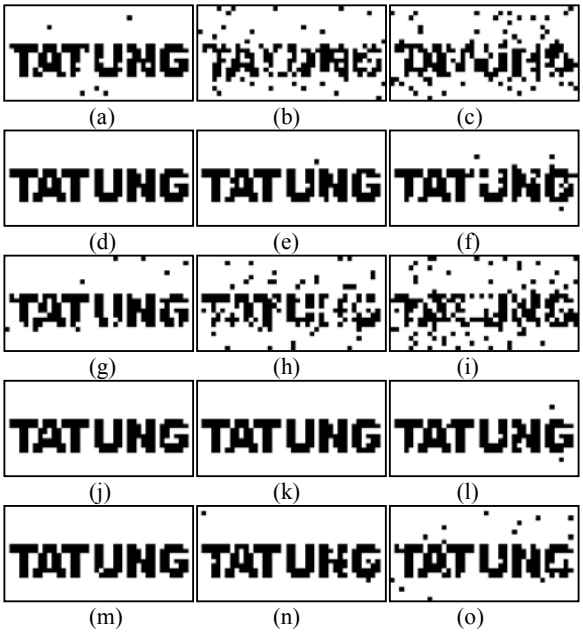

Fig. 7 The watermarks extracted from the watermarked "Boats" image which is embedded in the (a) YC_bC_r, (b) XYZ, and (c) CIELAB color spaces and attacked by the JPEG compression (CR=32.54); (d) YC_bC_r, (e) XYZ, and (f) CIELAB color spaces and attack by low-pass filtering; (g) YC_bC_r, (h) XYZ, and (i) CIELAB color spaces and added by zero-mean Gaussian noises with variance of 121.0; (j) YC_bC_r, (k) XYZ, and (l) CIELAB color spaces and scaled down by a factor of 4; (m) YC_bC_r, (n) XYZ, and (o) CIELAB color spaces and scaled up by a factor of 4.

$\mathbf{\Phi} = \{(\phi_1, \phi_2, ..., \phi_{n_z}) : \phi_k = 1, \text{or } 0, k = 1,2,3,..., n_z\}$, is created for embedding watermarks. This space consists of 2^{n_z} binary vectors to which each vector can be used for mapping. The 2^{n_z} binary vectors actually provide the space for carrying watermark information, and can be used as codes for representing each bit of the watermark. Through multiple ways of coding, each bit of the watermark can has more than one representations of codes. With different codes being assigned to represent the watermark, the watermark is expected to be more robust in that the signal is enabled to tolerate $(\Sigma n_Z)/2$ erroroneous bits. In the process of determining the watermarked location, perceptually significant coefficients are chosen for embedding the watermark.

Fig. 5 shows the original "Lena" image and its corresponding watermarked images, in each of which the watermark is embedded in the YC_bC_r, XYZ, and CIELAB space, respectively. In Fig. 6, the original "Goldhill" image and its corresponding watermarked images are shown. The indistinguishability between the original and its watermarked images shows that the embedded watermark is visually transparent no matter the embedding process is carried out in YC_bC_r, XYZ, or CIELAB space.

The bit error rate of the watermark that is extracted from the attack version of various watermarked image is shown in Table I. For the JPEG-compression attack, the watermark extracted from the watermarked "Lena", "Boats", "Goldhhill", and "Tulips" images is obtained at compression ratios of 38.40, 32.54, 33.59, and 25.00, respectively, while the watermark embedding is implemented in the YC_bC_r, XYZ, and CIELAB space, respectively. The bit error rate of the extracted watermark is the lowest for the watermarking scheme that is carried out in the YC_bC_r color space. Even though the compression ratio of the JPEG compression is as high as 38.40 for the watermarked "Lena" image, the bit error rate of the extracted watermark is lower than 5% when the watermark is embedded in the YC_bC_r color space. The robustness of the watermarking scheme exploiting the YC_bC_r and XYZ color spaces is higher than that exploiting the CIELAB color space while the watermarked image is attacked by the JPEG compression. It demonstrates that the YC_bC_r and XYZ color spaces have large amount of the perceptual redundancy for color pixels in this color space. The larger the extent of perceptual redundancy, the greater the strength of the watermark signal can be embedded, and the higher the robustness the embedded watermark may possess. For the attack by adding zero-mean Gaussian noises with variance of 121.0, the watermark embedded in the YC_bC_r and XYZ color spaces is more robust than that embedded in the CIELAB color space. In face of various attacks, Table I obviously shows that the watermark embedded in the non-uniform space (YC_bC_r and XYZ) is always robust than that embedded in the uniform space (CIELAB). The watermarks extracted from the watermarked "Boats" image that is attacked by various attacks are shown in Fig. 7. Fig. 7 (a), (b), and (c) show the watermarks extracted from the JPEG-compressed version of the watermarked images, in each of which the watermark is embedded in the YC_bC_r, XYZ, and CIELAB spaces, respectively. At a compression ratio of 32.54, it shows that the bit error rates of the extracted watermarks are only 1.88% and 9.65% using YC_bC_r and XYZ space, respectively, while the bit error rate of the extracted watermark is 13.13% using CIELAB space. Fig. 7 (d), (e), and (f) show the watermarks extracted from the watermarked images that are attacked by low-pass filtering. Fig. 7 (g), (h), and (i) show the watermarks extracted from the watermarked images that are attacked by adding zero-mean Gaussian noise. It is found that the watermark embedded in the YC_bC_r and XYZ space is more robust than that embedded in the CIELAB space when the watermarked image is contaminated by zero-mean Gaussian noises of variance 121. Fig. 7 (j), (k), and (l) show the watermarks extracted from the watermarked images that are scaled down by a factor of 4. Fig. 7 (m),

(n), and (o) show the watermarks extracted from the watermarked images that are scaled up by a factor of 4.

5. Conclusions

In this paper, robustness of the color image watermarking scheme using different color spaces for embedding is compared. The proposed watermarking scheme uses the perceptually redundant signal spaces to insert watermarks in color spaces. The robustness comparison shows that the non-uniform color spaces indeed provide a certain part of color signals a large amount of perceptual redundancy for embedding high-strength watermark signals which can always survive the attack. The choice of the color space for color image watermarking schemes is highly related with the corresponding robustness. The idea can be extended and applied to the video signal. Embedding watermarks into the perceptually redundant space of color video signals has been under investigation.

References

[1] R. B. Wolfgang, C. I. Podilchuk, and E. J. Delf, "Perceptual watermarks for digital images and video," *Proc. IEEE*, vol. 87, pp. 1108-1126, July 1999.

[2] I. J. Cox, J. Kilian, F. T. Leighton, and T. Shamoon, "Secure spread watermarking for multimedia," *IEEE Trans. Image Processing*, vol. 6, pp. 1673-1687, Dec. 1997.

[3] C. I. Podilchuk and W. Zeng, "Image-adaptive watermarking using visual models," *IEEE J. Select. Areas Commun*., vol. 16, pp. 525-539, May 1998.

[4] Chun-Shien Lu, Shih-Kun Huang, Chwen-Jye Sze, and Hong-Yuan Mark Liao, "Cocktail watermarking for digital image protection," *IEEE Trans. Multimedia*, vol. 2, pp. 209-224, Dec. 2000.

[5] M. Barni, F. Bartolini, and A. Piva, "Improved wavelet-based watermarking through pixel-wise masking," *IEEE Trans. Image Processing*, vol. 10, pp. 783-791, May 2001.

[6] M. Kutter and S. Winkler, "A vision-based masking model for spread-spectrum image watermarking," *IEEE Trans. Image Processing*, vol. 11, pp.16-25, Jan. 2002.

[7] M. Saito, M. Kino, and S. Wada, "HVS based wavelet watermarking with bit data embedded in color images," in *Proc. Int. Conf. on Communication Systems*, vol. 1, Nov. 2002, pp. 25-28.

[8] M. Kutter, F. Jordan, and F. Bossen, "Digital signature of color images using amplitude modulation," *J. Electron. Imag.*, vol. 7, pp. 326-332, 1998.

[9] D. J. Fleet and D.J. Heeger, "Embedding invisible information in color Images," in *Proc. IEEE Int. Conf. Image Processing*, Oct. 1997, pp.532-535.

[10] M. Caramma, R. Lancini, F. Mapelli, and S. Tubaro, "A blind & readable watermarking technique for color images," in *Proc. IEEE Int. Conf. Image Processing*, Sept. 2000, pp.442-445.

[11] H. J. Liu, X. G. Kong, X. D. Kong, and Y. Liu, "Content based color image adaptive watermarking scheme," in *Proc. IEEE Int. Conf. Circuits and Systems*, May 2001, pp.41-44.

[12] M. Barni, F. Bartolini, and A. Piva, "Multichannel watermarking of color images," *IEEE Trans. Circuits Syst. Video Technol.*, vol. 12, pp. 142-156, Mar. 2002.

[13] A. Parisis, P. Carre, C. Fernandez-Maloigne, and N. Laurent, "Color image watermarking with adaptive strength of insertion," in *Proc. IEEE Int. Conf. Acoustics, Speech, and Signal Processing*, May 2004, pp.85-88.

[14] P.S. Huang, C. S. Chiang, C. P. Chang, and T. M. Tu, "Robust spatial watermarking technique for colour images via direct saturation adjustment," *IEE Proc. Vision, Image and Signal Processing*, vol. 152, pp.561-574, Oct. 2005.

[15] C. H. Lin, D. Y. Chan, H. Su, and W. S. Hsieh, "Histogram-oriented watermarking algorithm: colour image watermarking scheme robust against geometric attacks and signal processing," *IEE Proc. Vision, Image and Signal Processing*, vol. 153, pp.483-492, Oct. 2006.

[16] C. H. Chou and T. L. Wu, "Embedding color watermarks in color images", *EURASIP Journal of Applied Signal Processing*, pp.32-40, vol. 1, Jan. 2003.

[17] G. Sharma and H. J. Trussell, "Digital color imaging," *IEEE Trans. Image Processing*, vol. 6, pp. 901-932, July 1997.

[18] M. Mahy, L. Van Eyckden, and A. Oosterlinck, "Evaluation of uniform color spaces developed after the adoption of CIELAB and CIELUV," *Color Res. Appl.*, vol. 19, pp. 105-121, Apr. 1994.

[19] D. L. MacAdam, "Specification of small chromaticity differences," *J. Opt. Soc. Am.*, vol. 33, pp. 18-26, 1943.

[20] X. Zhang and B. A. Wandell, "A spatial extension of CIELAB for digital color image reproduction," in *Proc. SID Symposium Technical Digest*, 1996, vol. 27, pp. 731-734.

[21] F. H. Imai, N. Tsumura, and Y. Miyake, "Perceptual color difference metric for complex images based on Mahalanobis distance," *Journal of Electronic Imaging*, Vol. 10, Issue 2, pp. 385-393, April 2001.

[22] M. D. Fairchild, *Color Appearance Models*, Addison Wesley Longman, Inc., 1998.

[23] C. H. Chou and Y. C. Li, "A perceptually tuned subband image coder based on the measure of just-noticeable-distortion profile," *IEEE Trans. Circuits Syst. Video Technol.*, vol. 5, pp. 467-476, Dec. 1995.

[24] Chun-Hsien Chou and Kuo-Cheng Liu, "A perceptually optimized JPEG-LS coder for color images," in *Proc. IASTED Int. Conf. on Signal Processing, Pattern Recognition, and Applications*, 2007, pp.26-32.

Kuo-Cheng Liu received the M.S. degrees in Department of Electrical Engineering, Tatung Institute of Technology, Taipei, Taiwan in 1995. In 1997, he joined the Department of Information Management at Taiwan Hospitality & Tourism College, Hualien, Taiwan, as a Lecturer. In 2005, he became an Assistant Professor at the Department of Information Management, Taiwan Hospitality & Tourism College, Hualien,

Taiwan. He is currently pursuing the Ph.D. degree at the Department of Electrical Engineering, Tatung University, where his research interests concern color image processing, image compression, and digital watermarking techniques.

Chun-Hsien Chou graduated from National Taipei Institute of Technology, Taipei Taiwan in 1979, and received the M.S. and Ph.D. degrees in electrical engineering from National Tsing Hua University, Hsinchu, Taiwan, in 1986 and 1990, respectively. In 1990, he joined the Department of Electrical Engineering at Tatung Institute of Technology, Taipei, Taiwan, as an Associate Professor. During the academic year from 1991 to 1992, he was a Postdoctoral Research member at AT&T Bell Laboratories, Murray Hill, NJ. In 1996, he became a Professor at the Department of Electrical Engineering, Tatung University, Taipei, Taiwan. His current research areas include color models of the human visual system, perceptual coding of color images, streaming video coding, virtual reality, and digital watermarking techniques.